Proc. Natl. Acad. Sci. USA
Vol. 94, pp. 2045–2049, March 1997
Physiology

Pore size of the malaria parasite's nutrient channel

SANJAY A. DESAI*† AND ROBERT L. ROSENBERG‡

*Division of Infectious Diseases and International Health, Duke University, Durham, NC 27710; and ‡Departments of Pharmacology and Physiology, Campus Box 7365, University of North Carolina, Chapel Hill, NC 27599

Communicated by Gerhard Giebisch, Yale University School of Medicine, New Haven, CT, January 3, 1997 (received for review, August 13, 1996)

ABSTRACT **The malaria parasite, *Plasmodium falciparum*, requires large amounts of nutrients to sustain its rapid growth within the human red blood cell. A recently identified ion channel on the surface of the intraerythrocytic parasite may provide direct access to these nutrients in the red blood cell cytosol. Evidence supporting this role was obtained by incorporating this channel into planar lipid bilayers. In bilayers, this channel has conductance and gating properties identical to the *in situ* channel, passes soluble macromolecules of up to 1400 Da, and functions as a high capacity, low affinity molecular sieve. These properties, remarkably similar to those of a pore on *Toxoplasma gondii* (another protozoan parasite causing human disease), suggest a novel class of channels used by these intracellular parasites to acquire nutrients from host cytosol.**

The intraerythrocytic malaria parasite acquires nutrients by endocytosis of red blood cell (RBC) cytosol (1), diffusion through a membranous duct (2), and/or direct access to RBC cytosol through a nutrient-permeable ion channel (3) on the parasitophorous vacuole membrane (PVM), the outer of two membranes that surround the parasite. This ion channel, identified by patch clamp of erythrocyte-free parasites, is present in high density and is permeable to amino acids and monosaccharides (3).

The physiological role of this PVM ion channel remains controversial for several reasons. First, patch clamp experiments using intact parasites (3) could not distinguish whether this channel spans only the PVM or both the PVM and the parasite plasma membrane, an underlying apposed membrane not accessible to the patch clamp pipette. This uncertainty has significant implications for how nutrients move from RBC cytosol into the parasite (4, 5); a channel spanning both membranes would obviate the need for additional transport pathways in the parasite plasma membrane but would deplete known Na^+ and K^+ gradients between parasite and RBC cytosols (6).

Second, patch clamp of the small intracellular parasite (~3 μm in diameter) is technically difficult and requires high concentrations of divalent cations (Ca^{2+} or Mg^{2+}), which may alter channel function. Although those experiments demonstrated that the channel is open >98% of the time at the PVM's resting membrane potential (3), open probabilities with more physiological solutions could not be determined. Indeed, the RBC's Ca^{2+}-activated K^+ channel is closed under physiological conditions but has a high open probability at micromolar Ca^{2+} concentrations (7).

Finally, the on-cell patch clamp configuration does not allow detailed biophysical characterization of the channel. For example, it could not determine the channel's affinity for permeating nutrients because it required near-isotonic pipette solutions. Furthermore, size restrictions on permeant molecules could not be examined.

To resolve these issues, we have incorporated this ion channel into planar lipid bilayers. In this method, channels are studied in a single bilayer without the second apposed bilayer that was present in the patch clamp experiments. This method also allows more complete manipulation of the bathing solutions on both sides of the bilayer, allowing detailed characterization of the channel.

MATERIALS AND METHODS

Culture and Preparation of Plasmodial Membranes. Indochina strain *Plasmodium falciparum*-infected RBCs were grown in RPMI 1640 culture medium with 10% human serum and 50 mg/l hypoxanthine (8), synchronized with sorbitol lysis (9), and harvested at the mid-trophozoite stage. Cells were lysed with 50 μg/ml digitonin at a hematocrit of 6% at 4°C in 100 mM KCl with buffer B (40 mM Hepes/10 mM EGTA/2.9 mM $CaCl_2$/2.0 mM $MgCl_2$/1.0 mM Na_2ATP/0.1 mM phenylmethylsulfonyl fluoride/1 μg/ml aprotinin/1 μg/ml leupeptin/1 μg/ml pepstatin A, pH 7.0 with KOH). Digitonin, a cholesterol-requiring detergent, permeabilizes RBC membranes without damaging parasite membranes or the nutrient channel (3). Parasites were then washed twice in the same solution without digitonin ($3000 \times g$, 5 min) before mechanical disruption with a Dounce homogenizer in buffer B without KCl at 4°C. The turbid supernatant was then centrifuged at $100{,}000 \times g$ for 30 min, and the pellet was resuspended in 100 mM KCl with buffer B before freezing in liquid nitrogen.

Incorporation into Planar Lipid Bilayers. Bilayers were formed from decane solutions of palmitoyl-oleoyl-phosphatidylethanolamine (15 mg/ml) and palmitoyl-oleoyl-phosphatidylserine (5 mg/ml) across a 200-μm-diameter hole (10). Bathing solutions on the two sides of the bilayer are given in the figure legends. Bilayers had resistances of 100–500 GΩ before channel incorporation. Parasite vesicles were thawed quickly and kept on ice until added to the cis chamber for incorporation into the bilayer, which occurred spontaneously within 5 min. The membrane potential, V_b, is defined as cis relative to trans. Single channel recordings were filtered at 200 Hz (8 pole Bessel) and digitized at 1 kHz.

Bathing Solution Conductivity Measurements. Polyethylene glycols (PEGs), added to the bathing solutions to determine channel pore size, decreased the conductivity of the solution as measured with a conductance bridge (model 31A, Yellow Springs Instruments). Addition of 20% (wt/vol) PEG (any polymer size) decreased the conductivity of the 100 mM KCl bathing solution from 12.6 to 6.9 mS/cm. A control PEG-free bathing solution with this same lower conductivity contained 55 mM KCl.

Chloride Activity Measurements. Addition of PEGs to the bathing solution also raised the K^+ and Cl^- activity coeffi-

The publication costs of this article were defrayed in part by page charge payment. This article must therefore be hereby marked "*advertisement*" in accordance with 18 U.S.C. §1734 solely to indicate this fact.

0027-8424/97/942045-5$2.00/0
PNAS is available online at **http://www.pnas.org**.

Abbreviations: RBC, red blood cell; PVM, parasitophorous vacuole membrane; PEG, polyethylene glycol.

†To whom reprint requests should be addressed at: Duke University Medical Center, Box 3824, Durham, NC 27710.

cients. This effect was quantitated by measuring the Cl^- activities with a Ag-AgCl electrode, a reference electrode (model 90–01, Orion, Boston), and a voltmeter. The Cl^- activity of the 100 mM KCl bathing solution was increased by 57% with addition of 20% (wt/vol) PEG (any size). Raising the KCl concentration to 160 mM produced the same increase in activity without adding PEGs.

RESULTS

Incorporation of the Nutrient Channel into Bilayers. Fig. 1*A* shows unambiguous single-channel events seen after incorporation of trophozoite membranes into planar lipid bilayers. With 100 mM monovalent charge carriers on both sides of the bilayer, these channels had a slope conductance of 155 pS and an apparent reversal potential, E_{rev}, of 9 mV (Fig. 1*B*, ●), in good agreement with the 140 pS and 2 mV seen for the nutrient channel *in situ* (3). Replacement of the charge carriers on the trans side of the bilayer with 240 mM glycine, a zwitterionic amino acid, decreased the conductance to 86 pS and shifted the E_{rev} by only −4 mV (Fig. 1*B*, ○), consistent with the 85 pS and −7 mV shift measured *in situ* (3). The small shift in E_{rev} indicates negligible cation or anion selectivity.

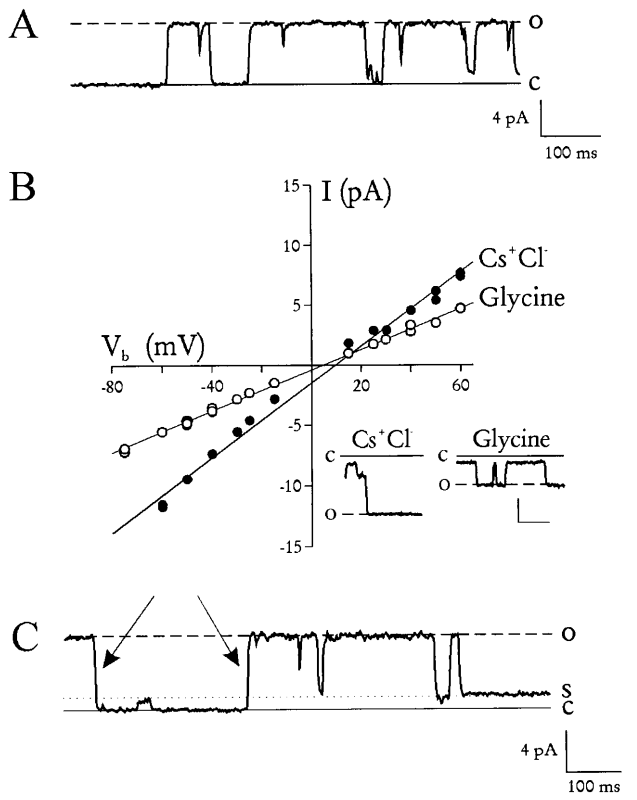

FIG. 1. Incorporation of the nutrient channel into planar lipid bilayers. (*A*) Channel activity seen after addition of parasite vesicles to planar lipid bilayers. Dashed and solid lines represent channel open and closed states, respectively. Bathing solution was designed to simulate RBC cytosol and contained (both sides) 100 mM KCl with buffer A (20 mM Hepes/2.0 mM $MgCl_2$/1 mM Na_2ATP, pH 7.3 with NaOH). V_b was +30 mV. (*B*) The channel's current–voltage relationship. Main figure shows unitary current amplitudes (measured by eye) plotted against V_b. The cis bathing solution was the same as that used in *A*. The trans solution contained either 100 mM CsCl + buffer A (●) or 240 mM glycine + buffer A (○). The decrease in slope conductance (from 155 to 86 pS) and the minimal change in E_{rev} (from +9 to +5 mV) upon replacement of CsCl with glycine confirm that these channels were equally permeable to cations, anions, and glycine, consistent with similar measurements on intact parasites (3). The slope conductances and the E_{rev} values were identical to those measured by patch clamp of intact parasites (3), confirming that this is the same channel. Channel events in CsCl (*Left Inset*) and glycine (*Right Inset*) at $V_b = -50$ mV. Scale, 4 pA/100 ms. (*C*) Subconductance states. Solid and dashed lines represent closed and fully open states, respectively. The dotted line represents a subconductance level seen previously (3). It is not a separate channel because there are two full transitions (indicated by arrows) that would require the unlikely simultaneous opening and closing of two independent channels. Bath solutions are the same as those in *A*. $V_b = +30$ mV.

Other biophysical properties, identical to those measured by patch clamp of the PVM, confirm that these channels reconstituted into planar lipid bilayers were the same nutrient-permeable channels studied by patch clamp (3). The reconstituted channels exhibited subconductance states (Fig. 1*C*) similar to those seen previously. They also had open probabilities >96% at near-zero membrane potentials and a bell-shaped voltage dependence (Fig. 2). These experiments, which used physiological divalent cation concentrations, demonstrate that the channel's high open probability was not an artifact produced by the high divalent cation concentrations required for the previous patch clamp experiments (3). In addition, the identical conductance and gating properties of the nutrient channel in bilayers also suggest that the channel's function does not depend significantly on its physical environment because the lipid composition of the bilayer differs markedly from that of the PVM (12).

This channel activity was never seen in bilayers without addition of parasite vesicles (n = 93) or with addition of identically prepared vesicles from uninfected RBCs (n = 61; data not shown). No other channel types were seen with incorporation of parasite vesicles.

Measurement of Pore Size. Although the nutrient channel is permeable to several large organomolecules (3), an upper size limit on permeation has not been established. We examined this size limit by adding PEGs of discrete polymer lengths to the bathing solution on both sides of the bilayer. PEGs are spherical in aqueous solutions and have been used to accurately measure other channel pore sizes (13, 14). We added PEGs ranging in size from 200 to 3350 Da and used changes

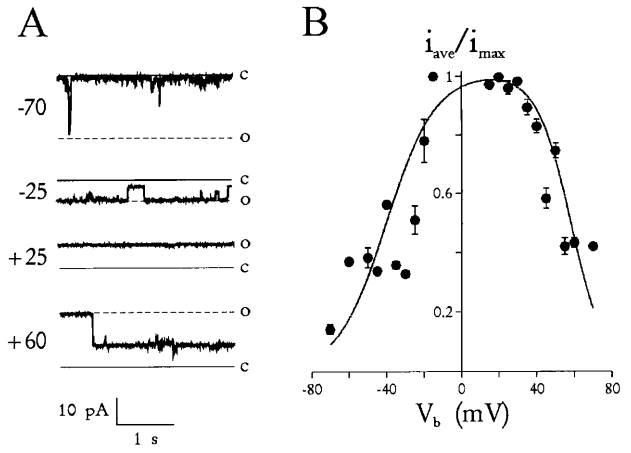

FIG. 2. Voltage dependence of the channel. (*A*) Typical channel activity at a range of V_b values indicated. The bathing solution on both sides of the bilayer was 160 mM KCl + buffer A. The channel's closed and fully open states are indicated by solid and dashed lines,respectively, at each voltage. Notice that the channel is mostly open at ±25 mV and less so at −70 and +60 mV. The intermediate level shown in the sweep recorded at +60 mV is a subconductance state. (*B*) Average normalized current as a function of V_b. At each V_b, recordings from the channel in *A* were integrated (average of 45 s each) and normalized to the value for a fully open channel. Although different from classical open probability determinations, this calculation incorporates transport during subconductance states and indicates the net flux per unit time. Notice that near $V_b = 0$, the channel passes ≥96% of its maximal current. The solid line is given by $i_{ave}/i_{max} = 1.01/\{[1 + \exp((-40 - V_b)/13)] \cdot [1 + \exp((V_b - 58)/9)]\}$, representing a fit to the product of two Boltzman equations (11).

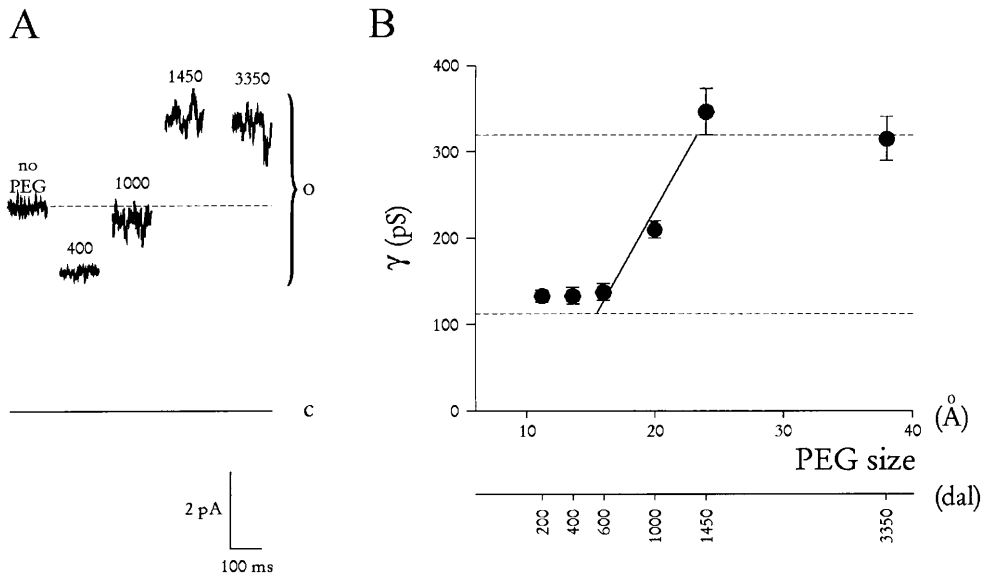

FIG. 3. Pore size of the nutrient channel. (*A*) Open amplitudes of single channels at $V_b = +25$ mV after addition of PEG. The bathing solution on both sides of the bilayer is 100 mM KCl with buffer A without (control) or with 20% (wt/vol) PEG (of indicated size). These channels are primarily open at this voltage (also seen in Fig. 2). Notice that the current amplitude increases with PEG size but reaches a maximum by PEG 1450. (*B*) Slope conductance of single channels (γ) vs. PEG diameter measured in water (15). ●, Average slope conductances ± SEM measured in 100 mM KCl with buffer A and 20% (wt/vol) PEG 200, 400, 600, 1000, 1450, and 3350 ($n = 3$ single channels each, ≥ 4 V_b values for each conductance). The dashed lines represents the average slope conductance measured in symmetric bathing solutions of 55 mM KCl/11 mM Hepes/1.1 mM $MgCl_2$/1 mM Na_2ATP, pH 7.3 (lower dashed line, $n = 2$ single channels) and 160 mM KCl/32 mM Hepes/3.2 mM $MgCl_2$/1 mM Na_2ATP, pH 7.3 (upper dashed line, $n = 4$ single channels). The solid line is a linear fit of the data for PEG 600, 1000, and 1450. It intercepts the upper dashed line at diameter of 23 Å, the estimated pore size of the channel.

in the channel's slope conductance, which measures permeation of charged ions (100 mM K^+ and Cl^- on both sides of the bilayer), to estimate the channel's pore size.

First, addition of small PEGs [≤400 Da, 20% (wt/vol)] caused a large decrease in open channel current (Fig. 3*A*). With PEG 400, the channel's slope conductance decreased from 210 ± 11 to 133 ± 10 pS (Fig. 3*B*) without a significant change in E_{rev} (data not shown). This decrease was quantitatively explained by a PEG-induced decrease in the conductivity of the bathing solution. Channels studied in a 55 mM KCl bathing solution without PEG, which has the same lower conductivity as 100 mM KCl plus 20% (wt/vol) PEG, had a slope conductance of 113 ± 14 pS (Fig. 3*B*, lower dashed line). Because this slope conductance was nearly identical to that measured in 100 mM KCl plus PEG 400, we conclude that PEG 400 permeates freely through the channel pore and decreases both channel conductance and bulk solution conductivity by hindering movement of K^+ and Cl^-.

Larger PEG polymers produced an identical decrease in bulk solution conductivity but decreased open channel current to lesser extents (Fig. 3*A*), reflecting incomplete channel permeation by these larger PEG molecules. The channel's slope conductance, at a minimum with PEG 200 and 400, increased with PEG size but reached a maximum value with the two largest PEGs tested, PEG 1450 and 3350. These two PEGs actually increased the channel's slope conductance above that without PEG (347 ± 27 and 316 ± 26 pS, respectively; Fig. 3). This initially unexpected observation results from the increased activity coefficients of K^+ and Cl^- in the presence of PEG, a phenomenon caused by a reduced bathing solution dielectric constant (16). To test if these largest PEGs are completely excluded from the channel, we compared these maximal channel slope conductances to those in a 160 mM KCl, PEG-free solution (320 ± 17 pS; Fig. 3*B*, upper dashed line), which had the same higher K^+ and Cl^- activities. The good agreement of these measurements indicates that PEG 1450 and 3350 cannot detectably permeate this channel because they produce the same channel slope conductance as the bathing solution without PEGs (allowing for effects on activity coefficients). Linear extrapolation (Fig. 3*B*, solid line) yields a size limit of 1400 Da on permeation and an effective channel pore diameter of 23 Å.

The Channel's Substrate Affinity. This large pore diameter could still produce slow fluxes if permeating substrates bind to a high affinity site in the channel during transport. We found that permeation does not involve a binding step because the channel slope conductance did not saturate with KCl concentrations up to 2 M (Fig. 4). This high, nonsaturating transport capacity suggests that this channel can be modeled as a rigid cylindrical sieve through which soluble macromolecules can pass, limited only by their diffusion coefficient in cytosol and a size in aqueous solution of less than 23 Å. For this simple model, the average diffusion coefficient and hydrated diameter of K^+ and Cl^- ions (75 S/cm/g-equivalent/cm^3 (17) and 3.6 Å (11), respectively) predict a slope for the conductance–concentration profile of 7.4 nS/M. This calculated value, within 3-fold of the measured 3.2 nS/M (slope of line in Fig. 4), suggests that the crude model of a water-filled pore is reasonable (cf. ref. 18).

DISCUSSION

We propose that the primary function of this channel is to provide the parasite access to soluble macromolecules in RBC cytosol. Monosaccharides (19), amino acids (20, 21), and purine nucleotides (21–23) in the RBC cytosol are taken up by the intracellular parasite to sustain its high metabolic rate. These precursors cross the PVM by diffusion through this channel and likely cross the underlying parasite plasma membrane via specific carriers, a two-step transport process analogous to that of mitochondria and Gram-negative bacteria. Saturable transport of macromolecules observed in erythrocyte-free parasites (19, 21, 23) therefore reflects the transport kinetics of the underlying plasma membrane because transport across the PVM is not likely to be rate-limiting. Additionally, plasmodial peptides present in the RBC cytosol may reach

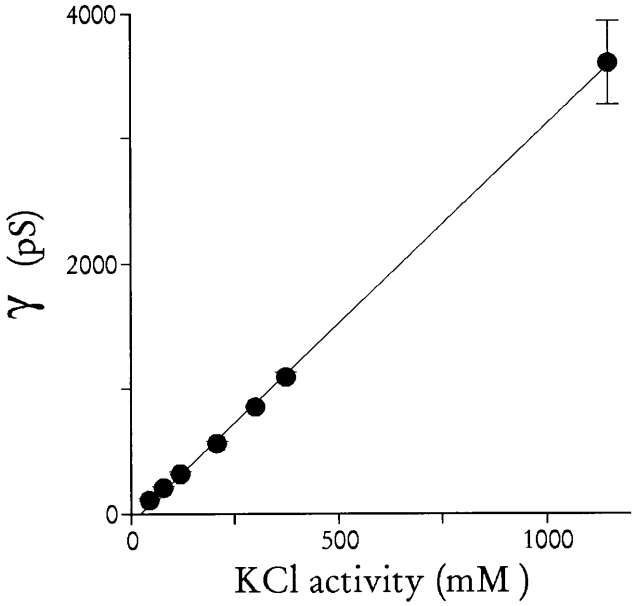

FIG. 4. Channel conductance vs. KCl concentration. Single channel slope conductances were determined in symmetric bathing solutions of buffer A with 55, 100, 160, 300, 455, 583, and 2000 mM KCl (n = 2, 5, 4, 2, 1, 3, and 3 single channels, respectively; $\geq$4 V_b values for each conductance). The average conductances with SEMs are here shown against the KCl activity (KCl concentration multiplied by tabulated activity coefficients; ref. 17). Notice that channel conductance does not saturate with increasing KCl concentrations.

their target by exocytosis at the parasite plasma membrane and subsequent threading through this PVM channel (24).

The channel's pore diameter of 23 Å (1400 Da) is larger than most porins on mitochondria and Gram-negative bacteria (10–20 Å; ref. 25) but smaller than the chloroplast porin (30 Å; ref. 26). The PVM of another intracellular parasite, *Toxoplasma gondii*, has an exclusion limit for fluorescent peptides of 1300 Da (27), in remarkable agreement with this plasmodial channel. Perhaps a class of related channels are used by these intracellular parasites to access soluble macromolecules in their host cytosol.

Patch clamp experiments using intact erythrocyte-free parasites could not determine whether this channel spans only one or both of the closely apposed membranes surrounding the parasite. Incorporation into a single lipid bilayer with identical conductance and gating properties (Figs. 1 and 2) strongly supports a channel configuration that spans only one membrane because a second juxtaposed membrane, needed for the alternative configuration, is not present in these experiments. In contrast, gap junction channels, which span two membranes, have properties markedly different from their source tissue when incorporated into single bilayers (28, 29).

A recently proposed membranous duct may provide the parasite direct access to serum by connecting the PVM to the RBC membrane (2). Coexistence of the nutrient channel with such a membranous duct is problematic because nutrients in the RBC cytosol could pass though the channel and leak into the extracellular space by diffusion down the ducts (4). The presence of these controversial ducts, identified by uptake of fluorescent dextrans, has not been confirmed by uptake of other large labeled molecules, electron microscopy, or diffusive exchange of lipids between the PVM and RBC membranes (30–32). Nevertheless, if the ducts do exist, they may exist only transiently (32), reducing the concern of RBC nutrient leakage.

Our data are most consistent with a pore-forming protein of parasitic origin. How might such a protein reach and be inserted into the PVM? It may be incorporated into the nascent PVM at the time of RBC invasion by a merozoite. The protein and lipid contents of secretory organelles in the merozoite (rhoptries) are discharged during invasion and likely contribute to the PVM (33). This mechanism of routing the channel to the PVM is appealing because nutrients in the RBC cytosol would become accessible to the parasite immediately after invasion. Alternatively, the channel may be packaged as a soluble protein in dense granules that are exocytosed into the space beneath the PVM soon after invasion (33). This protein may then be incorporated into the PVM by hydrophobic interactions, a mechanism with precedence in *Toxoplasma gondii* (34). Finally, the protein may be translated as an integral membrane protein that reaches the PVM by fusion of vesicles that bud from the parasite plasma membrane (35). Regardless of how these channels reach the PVM, regulatory mechanisms likely prevent channel-mediated transport until incorporation in the PVM because the large pore size would cause undesirable equilibration of solutes across other parasite membranes.

The nutrient channel was studied here by incorporation into planar lipid bilayers, a method with two advantages over previous patch clamp experiments (3). First, these experiments are not technically limited by the parasite's small size. Indeed, channels from other stages of the life cycle, which are too small for patch clamp, may be found only by incorporation into bilayers. Second, the bilayer method allows examination of possible channel blockers by addition to either or both faces of the incorporated channel. We found no effect on channel conductance or gating with three known antimalarial drugs (100 μM quinine, 100 μM chloroquine, or 0.3 μM artimisinin; data not shown). This channel, now more experimentally accessible, may be an ideal target for new antimalarial drugs.

We thank J. Hamilton, D. Krogstad, E. McCleskey, and A. VanDongen for their help and advice, and G. Cox and K. Joiner for reviewing the manuscript. This work was supported by the National Institute of Allergy and Infectious Diseases and the National Heart, Lung, and Blood Institute (National Institutes of Health, Bethesda).

1. Goldberg, D. E., Slater, A. F., Beavis, R., Chait, B., Cerami, A. & Henderson, G. B. (1991) *J. Exp. Med.* **173,** 961–969.
2. Pouvelle, B., Spiegel, R., Hsiao, L., Howard, R. J., Morris, R. L., Thomas, A. P. & Taraschi, T. F. (1991) *Nature (London)* **353,** 73–75.
3. Desai, S. A., Krogstad, D. J. & McCleskey, E. W. (1993) *Nature (London)* **362,** 643–646.
4. Ginsburg, H. (1994) *Biochem. Pharmacol.* **48,** 1847–1856.
5. Desai, S. A. (1994) *Parasitol. Today* **10,** 24.
6. Lee, P., Ye, Z., Van Dyke, K. & Kirk, R. G. (1988) *Am. J. Trop. Med. Hyg.* **39,** 157–165.
7. Christophersen, P. (1991) *J. Membr. Biol.* **119,** 75–83.
8. Trager, W. & Jensen, J. B. (1976) *Science* **193,** 673–675.
9. Lambros, C. & Vanderberg, J. P. (1979) *J. Parasitol.* **65,** 418–420.
10. Rosenberg, R. L., Hess, P. & Tsien, R. W. (1988) *J. Gen. Physiol.* **92,** 27–54.
11. Hille, B. (1992) *Ionic Channels of Excitable Membranes* (Sinauer, Sunderland, MA).
12. Hsiao, L. L., Howard, R. J., Aikawa, M. & Taraschi, T. F. (1991) *Biochem. J.* **274,** 121–132.
13. Mark, J. E. & Flory, P. J. (1965) *J. Am. Chem. Soc.* **87,** 1415–1422.
14. Krasilnikov, O. V., Sabirov, R. Z., Ternovsky, V. I., Merzliak, P. G. & Muratkhodjaev, J. N. (1992) *FEMS Microbiol. Immunol.* **105,** 93–100.
15. Scherrer, R. & Gerhardt, P. (1971) *J. Bacteriol.* **107,** 718–735.
16. Edsall, J. T. & Wyman, J. (1958) *Biophysical Chemistry* (Academic, New York).
17. Robinson, R. A. & Stokes, R. H. (1970) *Electrolyte Solutions* (Butterworth, London).
18. Stein, W. D. (1986) *Transport and Diffusion Across Cell Membranes* (Academic, Orlando, FL).
19. Tanabe, K. (1990) *Parasitol. Today* **6,** 225–229.
20. Trager, W. (1971) *J. Protozool.* **18,** 392–399.
21. Sherman, I. W. (1977) *Bull. W. H. O.* **55,** 211–225.
22. Hansen, B. D., Sleeman, H. K. & Pappas, P. W. (1980) *J. Parasitol.* **66,** 205–212.
23. Kanaani, J. & Ginsburg, H. (1989) *J. Biol. Chem.* **264,** 3194–3199.

24. Lingelbach, K. R. (1993) *Exp. Parasitol.* **76,** 318–327.
25. Benz, R. (1985) *CRC Crit. Rev. Biochem.* **19,** 145–190.
26. Flügge, U. I. & Benz, R. (1984) *FEBS Lett.* **169,** 85–89.
27. Schwab, J. C., Beckers, C. J. & Joiner, K. A. (1994) *Proc. Natl. Acad. Sci. USA* **91,** 509–513.
28. DeVries, S. H. & Schwartz, E. A. (1992) *J. Physiol.* **445,** 201–230.
29. Harris, A. L., Walter, A., Paul, D., Goodenough, D. A. & Zimmerberg, J. (1992) *Mol. Brain Res.* **15,** 269–280.
30. Haldar, K. & Uyetake, L. (1992) *Mol. Biochem. Parasitol.* **50,** 161–177.
31. Atkinson, C. T. & Aikawa, M. (1990) *Blood Cells* **16,** 351–368.
32. Pouvelle, B., Gormley, J. A. & Taraschi, T. F. (1994) *Mol. Biochem. Parasitol.* **66,** 83–96.
33. Haldar, K. & Holder, A. A. (1993) *Semin. Cell. Biol.* **4,** 345–353.
34. Ossorio, P. N., Duremetz, J. F. & Joiner, K. A. (1994) *J. Biol. Chem.* **269,** 15350–15357.
35. Günther, K., Tümmler, M., Arnold, H. H., Ridley, R., Goman, M., Scaife, J. G. & Lingelbach, K. (1991) *Mol. Biochem. Parasitol.* **46,** 149–158.